Hyper-scale analysis of surface roughness

John B. Lindsay, Daniel R. Newman
Geomorphometry and Hydrogeomatics Research Group,
Department of Geography, University of Guelph
Guelph, Canada, Email: jlindsay@uoguelph.ca

Abstract—**Surface roughness is frequently measured using DEMs to characterize the ruggedness and topographic complexity of landscapes. Roughness maps have been applied in geological mapping, ecological modeling, and other environmental applications. These maps are typically derived using a roving-window approach, where kernel size dictates the scale at which roughness is assessed. The pattern of roughness is strongly scale dependent and this roughness-scaling relation can reveal useful information about the geomorphologic character of landscapes. This study applied hyper-scale analysis of a normal-vector based roughness metric for a LiDAR DEM of Rondeau Bay, Canada. The use of integral images, a data structure for computationally efficient filtering operations, allowed for the fine scale resolution of the analysis. The unique roughness scale signature of each grid cell in the DEM was derived for all spatial scales ranging from 3 to 5000 cells (7.5 m to 12,502.5 m). Maps of maximum roughness and the scale of maximum roughness were created for the study site. This cell-specific scaling approach to the characterization of surface roughness is in contrast to the use of single, often arbitrarily selected, kernel sizes to map topographic attributes. The additional information provided by the scale map was found to provide valuable ancillary data for landscape interpretation.**

I. INTRODUCTION

Surface roughness is a common topographic attribute measured from DEMs. A range of DEM-derived surface roughness metrics have been widely applied in geoscience and environmental research [1], [2]. For example, roughness maps have been used to delineate large-scale geological units on the moon [3] and Mercury [4]. Glenn et al. [5] applied surface roughness mapped from a fine-resolution LiDAR DEM to characterize the Salmon Falls landslide in Idaho. Roughness has also been widely applied in the study of fire behavior [1], [6].

Roughness maps are derived by measuring topographic variability within the local neighborhood surrounding each grid cell in a DEM. Thus, roughness is commonly mapped using the same roving-window approach used for many topographic attributes. The size of the local neighborhood dictates the scale at which surface roughness is characterized and will significantly impact the resulting roughness map. The scale-variant nature of roughness is widely recognized in the literature [2], [3], [7]. Ideally, roughness is assessed at a scale that is meaningful with respect to the scale of landforms, geomorphological processes, and the application. Ultimately, for heterogeneous landscapes, a single optimal scale cannot be defined to measure surface roughness. Rather, a range of scales are more appropriate for capturing the varying complexity of the topographic surface in a region. This has led some researchers to study the multi-scale properties of topographic surface roughness [2], [7].

Grohmann et al. [2] used a combination of filtering, based on varying sized kernels, and data resampling (i.e. DEM grid coarsening) to study roughness for a site in Scotland across a wide range of spatial scales. They concluded that the computational time required to calculate roughness using large kernel sizes is problematic for multi-scaled analysis. Data coarsening methods can improve the computational efficiency of these operations, but at the cost of losing some topographic information. More recently, [8] and [9] showed how efficient filtering methods based on integral images [10] can be applied to measures of local topographic position (LTP), allowing for efficient 'hyper-scale' (analogous to hyper-spectral) analysis of topographic properties. This paper extends these earlier studies to examine the hyper-scale properties of topographic roughness.

II. ROUGHNESS MEASURES

A large number of roughness metrics have been devised and previously applied in the literature. In part, this reflects the fact that at least two different but related concepts are often conflated in common usage of the term surface roughness. First, roughness can refer to local *elevation variability*. Elevation range (relief), standard deviation in elevation, and standard deviation of topographic residuals are common metrics used to characterize elevation variability. This dimension of the roughness concept will be referred to as *ruggedness*. The second aspect of roughness is *surface complexity*, a measure of topographic texture. Roughness metrics that characterize texture either use surface area (e.g. topographic roughness index [1]), or surface normal vectors (or components of normals, e.g. slope and aspect). Vector

dispersion and standard deviation of slope have been used previously to characterize surface complexity [2]. Notice that relatively flat, smooth surfaces can exhibit high ruggedness (e.g. a plateau) and areas of complex texture can exhibit relatively low relief (e.g. the micro-topography of an agricultural field).

The scale-dependency of ruggedness is in part a result of the increased likelihood of including more prominent regional elevation minima and maxima with more extensive kernels. As a result, ruggedness maps tend to highlight elevation minima/maxima and breaks-in-slope, and ruggedness scale signatures (i.e. relation between roughness and kernel size) tend to be simple, monotonically increasing, non-linear functions. By comparison, the scale signatures for texture-based roughness metrics are generally more complex and are often indicative of variation in the topographic expression of geological units and their age.

III. METHODS

A. *Hyper-scale surface roughness measurement*

Working in the field of 3D printing, Ko [11] described surface roughness as the angular deviation between a surface's normal vectors and the normals of a corresponding ideal (i.e. smoothed) surface. This measure of surface complexity is therefore in units of degrees. Specifically, roughness is defined in this study as the neighborhood-averaged difference in the normal vectors of the original DEM and a smoothed DEM surface. Smoothed surfaces were derived by applying a mean filter of the same size as the neighborhood. Estimating normal vectors is a small local neighborhood operation, and therefore computationally more efficient than the extended neighborhood operation needed to smooth the DEM with varying and large kernel sizes. However, an integral image approach was used in this study to improve the computational efficiency of the smoothing operation.

An integral image is a raster data structure in which each grid cell's value represents the sum of an underlying distribution (a DEM in this case) within the rectangular area bounded by the cell and one of the image corners (usually the upper left corner). Widely applied in the field of computer vision, integral images allow for efficient four-operation measurements of the total of the underlying distribution for arbitrary sized rectangular areas. This can facilitate image filtering with computational efficiency varying with the number of grid cells in the image, but independent of the size the filter kernel. This is the basis for efficient, hyper-scale geomorphometric analysis proposed by [8]. Integral images must be calculated sequentially, because each value in grid cell depends on previous cells; however, integral-image based filtering operations are readily parallelized for further improved efficiency. Similarly, calculation of local normal vectors can also be parallelized. Two hyper-scale roughness plugin tools were implemented in the open-source WhiteboxTools library using the Rust programming language. The first tool (MultiscaleRoughnessSigature) was used to measure and plot the roughness metric at point locations across a specified range of spatial scales; the second tool (MultiscaleRoughness) mapped the pattern of maximum roughness, and the scale at which maximum roughness occurred, for each cell.

Note that in addition to window totals and averages, integral images can also be used to efficiently measure standard deviations within moving windows. As such, many other common roughness metrics (e.g. standard deviation in elevation, standard deviation in topographic residuals, standard deviation in slope, vector dispersion, and area ratio) are all conducive to the approach used in this study. Elevation range is the only one of the common roughness metrics that is poorly suited to measurement using integral images, since this method cannot measure window min/max values. Newman et al. [9] present other efficiency-optimized filtering techniques that could be used in this case.

B. *Study Site and DEM*

Scale-variant roughness patterns were evaluated for a 8026 × 8125 rows by columns, 2.5 m resolution LiDAR DEM of the Rondeau Bay area, located in Southwestern Ontario, Canada, along the northern coast of Lake Erie (Fig. 1). The Blenheim moraine transects the study site. McGregor Creek, a tributary of the Thames River, drains the region north of the moraine towards Lake St. Clair. The morainal ridge rises approximately 20 m above its surroundings. Drainage systems on the moraine are poorly organized owing to the hummocky topography. The area south of the moraine drains into Rondeau Bay through a series of deeply incised stream channels arranged in a parallel drainage pattern. The bay is sheltered from Lake Erie by Rondeau Spit, which consists of a tightly packed series of low, parallel sand ridges and dunes. Agriculture is the dominant land use in the site, although the spit is largely forested, and some smaller urbanized areas are also present, including the towns of Blenheim and Ridgetown (Fig. 1). The DEM was interpolated from last- and only-returns of the LiDAR point clouds, excluding early-returns and points classified as vegetation and buildings. An inverse-distance-weighting (IDW) scheme was used for interpolation. Several major roads transect the site, and their embankments are apparent in the DEM. While buildings were excluded from the interpolation, the urban areas are marked in the DEM by their differing texture. The dataset is irregular in extent; large no-data voids (white areas in Fig. 1) occur within the water bodies (Rondeau Bay) and in the areas to the southwest and northeast. While the overall relief is low-to-moderate, a range of surface

textures result from the variety of topographies within the areas of the moraine, spit, and incised fluvial dissection. This character makes the dataset well-suited to the purpose of studying surface roughness.

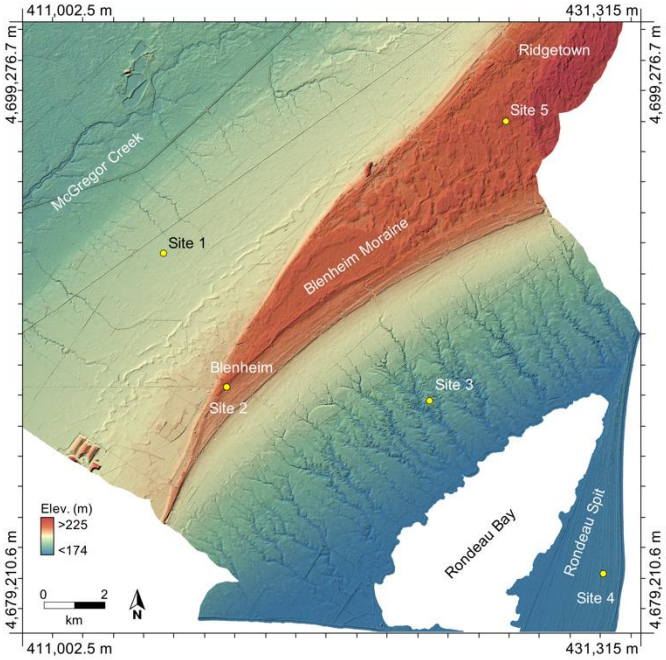

Figure 1. Hillshaded 2.5-m LiDAR DEM of the Rondeau Bay study site.

IV. Experimental Results

The surface roughness tools processed the test DEM in 59 min. using a dual-core 3.3 GHz processor. Fig. 2 presents the roughness scale signatures for the five sites identified in Fig. 1. Site 1 (flat agricultural area north of the moraine) was the only site with a signature that did not contain at least one peak. Sites 2 (urban) and 3 (area of incised channels) both experienced peak roughness with filter kernels in the range of 220-400 cells (550-1000 m). Site 3, located on the sand spit, possessed the highest peak (3.18°) and peaked at a relatively short spatial scale (15 cells; 37.5 m). Site 5 (hummocky terrain on the moraine) demonstrated one sharp and high peak at short spatial scales (55 cells; 137.5 m) and another broad, low peak at around 1500 cells (3750 m). Most of the variability in the scale signatures of the test sites occurred at scales less than 1000 cells (2500 m).

Fig. 3 shows the pattern of surface roughness in the Rondeau Bay site. This roughness map is unlike others reported in the literature, in that it does not represent the surface complexity at a single spatial scale; instead, it shows the peak roughness value of the unique scale signature associated with each grid cell. That is, Fig. 3 is a product of an amalgamation of scales, where each grid cell is represented at the scale of maximum roughness for the local topography within the broad range of tested scales. Fig. 4 maps the scale at which maximum surface roughness occurs for each cell.

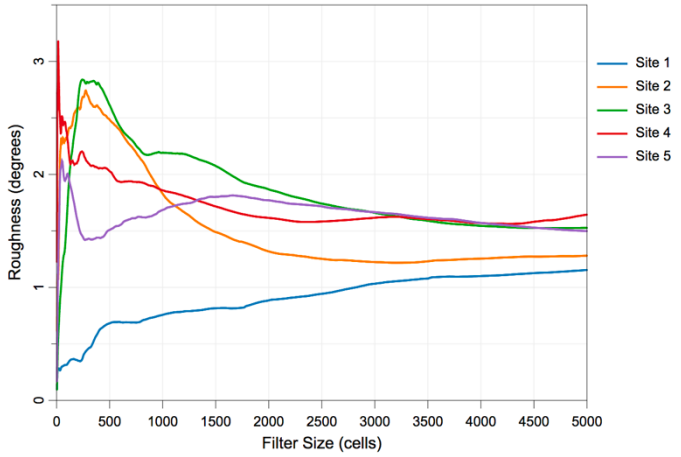

Figure 2. Roughness scale signatures for study sites (locations in Fig. 1). The range of filter sizes from 3 × 3 to 5000 × 5000 (7.5 m to 12,502.5 m).

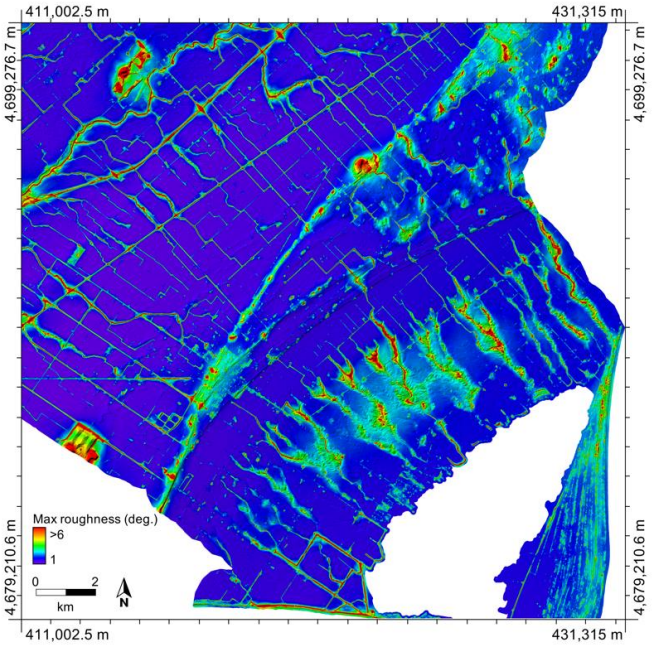

Figure 3. Maximum surface roughness (degrees) measured with filter sizes ranging from 3 to 5000 cells.

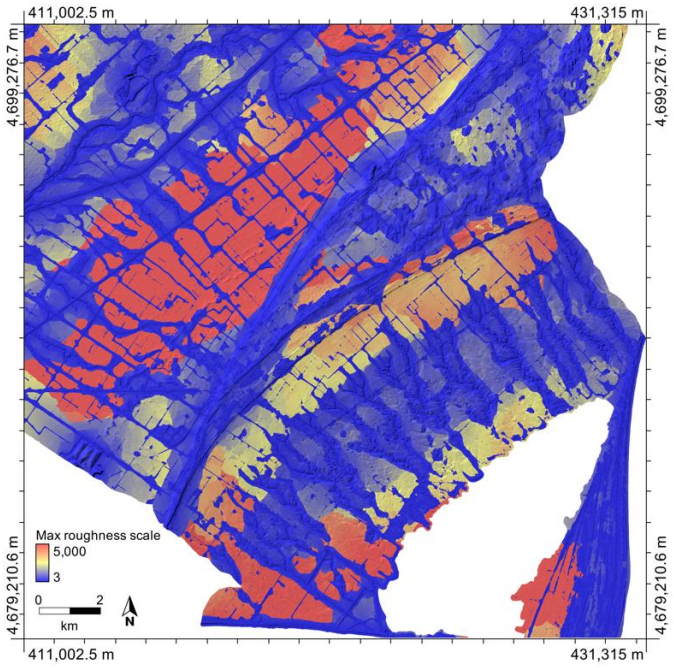

Figure 4. Filter size (i.e. spatial scale) of maximum surface roughness.

V. Discussion and Conclusions

The combination of the maximum roughness (Fig. 3) and the scale of maximum roughness (Fig. 4) aid in the interpretation of topographic properties of the study site. Areas of relatively high roughness were associated with the upper sections of the moraine, the two urban areas, the incised channels, the regions of low ridges on the sand spit, and all road embankments. Within the relatively smooth planar region in the northern section of the study site, broad stretches of low roughness were punctuated by locally high values associated with incised channels and roads. The impact of road embankments emphasizes the importance of removing these features from fine-resolution LiDAR DEMs in some applications. The region of tightly packed sand ridges along the eastern shoreline of Rondeau spit was associated with an extensive area of moderate to high values of roughness. The surface mounds of a landfill site, situated along the southwestern edge of the area, was also particularly apparent in the roughness map.

The mosaic of spatial scales associated with maximum roughness (Fig. 4) reveals substantial information about the topographic character of the test DEM. The widely ranging values of maximum roughness show that there is no single optimal kernel size that can be chosen to characterize topographic texture in a complex and extensive area. Interestingly, areas of high roughness were associated with shorter spatial scales and vice versa. The contrasting scales shown in Fig. 4 could provide additional information in geological mapping applications.

To conclude, this study demonstrated an application of the integral-image approach to measure surface roughness (topographic complexity) across a broad range of spatial scales with extremely fine scale resolution. This method allows for the characterization of maximum surface roughness at spatial scales that are optimal for each individual grid cell within a DEM. The information contained within the scale map can provide additional useful information for landscape interpretation.

Acknowledgment

Funding for this research was provided by the Natural Sciences and Engineering Research Council of Canada (NSERC).

References

[1] M. C. Stambaugh and R. P. Guyette, “Predicting spatio-temporal variability in fire return intervals using a topographic roughness index,” *For. Ecol. Manag.*, vol. 254, no. 3, pp. 463–473, 2008.

[2] C. H. Grohmann, M. J. Smith, and C. Riccomini, “Multiscale analysis of topographic surface roughness in the Midland Valley, Scotland,” *IEEE Trans. Geosci. Remote Sens.*, vol. 49, no. 4, pp. 1200–1213, 2011.

[3] M. A. Kreslavsky *et al.*, “Lunar topographic roughness maps from Lunar Orbiter Laser Altimeter (LOLA) data: Scale dependence and correlation with geologic features and units,” *Icarus*, vol. 226, no. 1, pp. 52–66, 2013.

[4] M. A. Kreslavsky, J. W. Head, G. A. Neumann, M. T. Zuber, and D. E. Smith, “Kilometer-scale topographic roughness of Mercury: Correlation with geologic features and units,” *Geophys. Res. Lett.*, vol. 41, no. 23, pp. 8245–8251, 2014.

[5] N. F. Glenn, D. R. Streutker, D. J. Chadwick, G. D. Thackray, and S. J. Dorsch, “Analysis of LiDAR-derived topographic information for characterizing and differentiating landslide morphology and activity,” *Geomorphology*, vol. 73, no. 1–2, pp. 131–148, 2006.

[6] D. Foster and G. King, “Vegetation pattern and diversity in SE Labrador, Canada: Betula papyrifera (birch) forest development in relation to fire history and physiography,” *J. Ecol.*, pp. 465–483, 1986.

[7] K. L. Frankel and J. F. Dolan, “Characterizing arid region alluvial fan surface roughness with airborne laser swath mapping digital topographic data,” *J. Geophys. Res. Earth Surf.*, vol. 112, no. F2, 2007.

[8] J. Lindsay, J. Cockburn, and H. Russell, “An integral image approach to performing multi-scale topographic position analysis,” *Geomorphology*, vol. 245, pp. 51–61, 2015.

[9] D. Newman, J. Lindsay, and J. Cockburn, “Evaluating metrics of local topographic position for multiscale geomorphometric analysis,” *Geomorphology*, In press.

[10] F. C. Crow, “Summed-area tables for texture mapping,” in *ACM SIGGRAPH computer graphics*, 1984, vol. 18, pp. 207–212.

[11] M. Ko, H. Kang, J. ulrim Kim, Y. Lee, and J.-E. Hwang, “How to Measure Quality of Affordable 3D Printing: Cultivating Quantitative Index in the User Community,” in *International Conference on Human-Computer Interaction*, 2016, pp. 116–121.